CELLULAR REPROGRAMMING
Volume 16, Number 2, 2014

DOI: 10.1089/cell.2013.0069

Brief Communication

Improving Viability and Transfection Efficiency with Human Umbilical Cord Wharton's Jelly Cells Through Use of a ROCK Inhibitor

Adam J. Mellott, BS,[1] Megan E. Godsey, BS,[2] Heather E. Shinogle, BA,[3] David S. Moore, PhD,[3] M. Laird Forrest, PhD,[4] and Michael S. Detamore, PhD[1,5]

Abstract

Differentiating stem cells using gene delivery is a key strategy in tissue engineering and regenerative medicine applications. Nonviral gene delivery bypasses several safety concerns associated with viral gene delivery; however, leading nonviral techniques, such as electroporation, subject cells to high stress and can result in poor cell viabilities. Inhibition of Rho-associated coiled-coil kinase (ROCK) has been shown to mitigate apoptotic mechanisms associated with detachment and freezing of induced pluripotent stem cells and embryonic stem cells; however, inhibiting ROCK in mesenchymal stromal cells (MSCs) for improving gene delivery applications has not been reported previously. In this study, we hypothesized that ROCK Inhibitor (RI) would improve cell viability and gene expression in primary human umbilical cord mesenchymal stromal cells (hUCMSCs) when transfected via Nucleofection™. As hypothesized, the pre-treatment and post-treatment of hUCMSCs transfected via nucleofection with Y-27632-RI significantly improved survival rates of hUCMSCs and gene expression as measured by green fluorescent protein intensity. This study provides the first comparative look at the effect of Y-27632-RI on hUCMSCs that underwent transfection via nucleofection and shows that using Y-27632-RI in concert with nucleofection could greatly enhance the utility of differentiating and reprogramming hUCMSCs for tissue engineering applications.

Introduction

Many tissue engineering strategies employ gene delivery approaches to differentiate stem cells toward terminal lineages (Jang et al., 2004; Kofron and Laurencin 2006; Shin et al., 2010; Zhang and Godbey 2006). While viral gene delivery remains popular for many tissue engineering applications due to high efficiency, concerns regarding toxicity, immunogenicity, and oncogenesis from insertional mutagenesis still remain (Check 2005; Thomas et al., 2003). Nonviral vectors are an alternative to viral vectors and in many cases are able to circumvent the safety concerns associated with viral vectors. However, in primary cells and stem cells, nonviral vectors usually exhibit low transfection efficiencies compared to their viral vector counterparts (Mellott et al., 2013). Significant technological advancements have been made in the last decade regarding electroporation that have led to increased transfection efficiencies, but low cell viabilities (Andre and Mir, 2010; Ear et al., 2001; Golzio et al., 2010). Thus, a method is needed that will enable primary cells and stem cells to be transfected at a high efficiency while maintaining acceptable cell viabilities for tissue engineering applications.

Over the past 5 years, several observations have been made regarding stem cell apoptosis related to detachment and freezing protocols as related to RhoA guanosine triphosphate (GTP) signaling pathways (Ohgushi and Sasai 2011; Xu et al., 2012; Zhang et al., 2011; Zhang et al., 2013). In particular, several research groups have noted that inhibition of the Rho-associated coiled-coil kinase (ROCK) appeared to increase cell survival by mitigating negative effects associated with cell dissociation and thawing (Claassen et al., 2009; Emre et al., 2010; Gauthaman et al., 2010a; Gauthaman et al., 2010b; Shi et al., 2013). The Y-27632 ROCK Inhibitor (Y-27632-RI) appeared to be especially useful for improving stem cell viability in human

[1]Bioengineering Program, University of Kansas, Lawrence, KS, 66045.
[2]Department of Biomedical Engineering, Duke University, Durham, NC, 27708.
[3]Microscopy and Analytical Imaging Lab, University of Kansas, Lawrence, KS, 66045.
[4]Department of Pharmaceutical Chemistry, University of Kansas, Lawrence, KS, 66047.
[5]Department of Chemical and Petroleum Engineering, University of Kansas, Lawrence, KS, 66045.

induced pluripotent cells (iPSCs) and embryonic stem cells (ESCs) (Joo et al., 2012; Narumiya et al., 2000). Furthermore, the use of Y-27632-RI was shown not to affect the pluripotency of ESCs (Watanabe et al., 2007). Chatterjee et al. (2011) were the first group to use RI to aid in the transfection of human iPSCs via Nucleofection™, an electroporative technique developed by Lonza Group Ltd. (Basel, Switzerland).

Human umbilical cord mesenchymal stromal cells (hUCMSCs) have a number of advantages over other cell sources and hold great potential for clinical translation, as we have reviewed extensively (Bailey et al., 2007a; Wang et al., 2009). Unfortunately, hUCMSCs are difficult to transfect, and few studies are available on the transfection of hUCMSCs. On the basis of its aforementioned success in other applications, we hypothesized that Y-27632-RI would improve cell viability and transfection efficiency for hUCMSCs that are transfected via nucleofection. In this study, transfection efficiency, gene expression, and cell viability were evaluated for hUCMSCs transfected via nucleofection with green fluorescent protein (GFP), with or without Y-27632-RI.

Materials and Methods

Procurement and expansion of hUCMSCs

hUCMSCs were isolated from Wharton's jelly of human umbilical cords obtained from the Kansas University Medical Center Hospital (IRB# 10951), Lawrence Memorial Hospital (IRB# LMH 08-2), and Stormont-Vail Hospital (IRB approved, no reference number) for a total of five cords used in the study ($n=5$). Four cords were from males that were born at full term and one cord was from a female born at 38.3 weeks, all under normal delivery conditions. Maternal age was not available. We isolated hUCMSCs according to our previous published protocol (Devarajan et al., 2013). hUCMSCs were cultured in traditional hUCMSC medium [10% fetal bovine serum (FBS-MSC Qualified) and 1% penicillin-streptomycin in low glucose Dulbecco's Modified Eagle Medium (DMEM); Life Technologies, Grand Island, NY, USA)]. hUCMSC medium was changed three times per week, and hUCMSCs were maintained at 37°C with 5% CO_2 in a cell culture–grade incubator. hUCMSCs were trypsinized with 0.05% trypsin-EDTA (1×) (Life Technologies) at 80–90% confluency. All hUCMSCs were expanded to passage 2 (P2) for the experiments. Five umbilical cords ($n=5$) in total were used for this study. All experiments were performed in triplicate for each cord.

Cell characterization

At P2, a subculture of cells from each cord was characterized through cell-surface marker identification via flow cytometry on a MoFlo XDP fluorescence-activated cell sorter (FACS) (Beckman Coulter, Brea, CA, USA). hUCMSCs were characterized using the following antibodies and secondary antibodies: STRO-1 mouse immunoglobulin M (IgM) (2.5:200; 1 mg/mL; R&D Systems, Minneapolis, MN, USA); Alexa Fluor 568® rabbit anti-mouse IgG (2:200; 2 mg/ mL; Life Technologies); CD105 mouse IgG (2.5:200; 1 mg/mL; R&D Systems); Qdot® 525 donkey anti-mouse IgG (2:200; 1 μM; Life Technologies); human CD45 preconjugated to Qdot® 800 (2:200; Life Technologies); human CD73 preconjugated to fluorescein isothiocyanate (FITC) (5:200; BD Biosciences, San Jose, CA, USA); human CD34 preconjugated to Brilliant Violet (5:200; BD Biosciences); human CD90 preconjugated to allophycocyanin (APC) (5:200; BD Biosciences). A total of 20,000 events were recorded for each sample. Positive identification of cell markers was defined as fluorescent emission that exceeded the fluorescent threshold of cells stained with corresponding isotype (negative) controls. The isotype controls used in these studies were rabbit IgG Alexa Fluor 568, donkey IgG Qdot 525, IgG_2 Qdot 800 (all from Life Technologies), and IgG_1 FITC, IgG_1 Brilliant Violet, and IgG_1 APC (all from BD Biosciences). The cell characterization experiments were repeated three times for each cord.

RI treatments and transfection

On the day of transfection, medium from all wells was removed, and cells were washed twice with phosphate-buffered saline (PBS). Afterward, cells were incubated for 1 h at 37°C in traditional hUCMSC medium (10% FBS-MSC Qualified/1% penicillin-streptomycin/low-glucose DMEM) or traditional hUCMSC medium with 10 μM of Y-27632-RI (Reagents Direct, Encinitas, CA, USA). After 1 h, hUCMSCs were washed twice with PBS, trypsinized, and then resuspended in 95 μL of 4D Nucleofector™ P1 Primary Solution (P1PS) (Lonza) at a density of 500,000 cells per 95 μL in a 50-mL conical tube (Phenix Research Products, Candler, NC, USA). 5 μL of P1PS or 5 μL of pmaxGFP (1 mg/mL; Lonza) was added to each sample, depending on the group, to bring the final cell suspension volume to 100 μL. hUCMSCs were separated into five groups consisting of three replicates per group. Groups 1 and 3 received no pmaxGFP. Groups 2, 4, and 5 each received 5 μL of pmaxGFP (1 mg/mL; Lonza). Groups 1, 2, 3, and 4 were cultured in traditional hUCMSC medium before and after transfection, while Group 5 was cultured in traditional hUCMSC medium with 10 μM of Y-27632-RI (Reagents Direct) before and after transfection. Our preliminary experiments revealed that a concentration of 10 μM of Y-27632-RI used both before and after transfection were preferred for effective transfection. hUCMSC suspensions from Groups 1 and 2 were immediately transferred to six-well plates (BD Biosciences) containing 1.5 mL of traditional hUCMSC medium and incubated at 37°C. hUCMSC suspensions from Groups 3, 4, and 5 were transferred to 100-μL 4D Nucleofection™ cuvettes. Each cuvette was gently tapped twice and then placed in a 4D Nucleofector™ (Lonza) and nucleofected with the program FF-104. hUCMSCs were incubated at room temperature (~22°C) for 10 min and then transferred to a six-well plate (BD Biosciences) containing 1.5 mL of traditional hUCMSC medium (Groups 3 and 4) or traditional hUCMSC medium with 10 μM of Y-27632-RI (Reagents Direct) (Group 5) and incubated at 37°C.

Fluorescent microscopy

At 24 h and 48 h after transfection, hUCMSCs were collected for analysis. A 0.5-μL amount of Hoechst 33342 dye (Life Technologies) was added to each well, and hUCMSCs were incubated for 10 min at 37°C. Afterward, hUCMSCs were imaged using an Olympus IX81 inverted epifluorescence microscope (Olympus America, Center Valley, PA, USA) with an Olympus LUCPlanFL 20X 0.4 NA

objective (Olympus). Images were captured using the software, SlideBook (Intelligent Imaging Innovations (3i), Denver, CO, USA). A mercury arc lamp was used with the following excitation filters (Excitation/Emission) for image collection: Hoechst (387 ± 11 nm/447 ± 60 nm) and GFP (494 ± 20 nm/531 ± 22 nm). For each sample that was imaged, a montage was generated from 25 (five by five arrangement) neighboring fields of view that were aligned together to generate one comprehensive composite image of the sample. All experiments were repeated three times for each umbilical cord at 24 h and 48 h.

FACS analysis

Immediately after imaging, cells were washed twice, trypsinized, and transferred into 5-mL polypropylene round-bottomed tubes (BD Biosciences). A 0.5-μL amount of propidium iodide (PI) (1 mg/mL; Life Technologies) was added to each sample just before analysis. hUCMSCs were analyzed via flow cytometry on the Beckman Coulter MoFlo XDP FACS. A total of 20,000 events were recorded for each sample analyzed. Flow cytometry was used to analyze both cell viability and transfection efficiency. Live hUCMSCs were characterized as hUCMSCs expressing Hoechst at an intensity of 10^2 relative fluorescence units (RFU) or above, with expression of PI at an intensity below 10^0 RFU. Dead hUCMSCs were characterized as hUCMSCs that expressed Hoechst at an intensity below 10^2 RFU and expressed PI at an intensity of above 10^0 RFU. GFP-positive hUCMSCs were characterized as live hUCMSCs that expressed GFP at an intensity of 10^0 RFU or greater. Transfection efficiency was determined by dividing the number of live GFP-positive cells in a sample by the total population of the sample. All experiments were repeated three times for each cord at 24 h and 48 h post-transfection. An example of how cell populations were gated is provided in Figure 1 and the statistics for all samples from an entire umbilical cord are displayed in Table 1.

Statistics

All values are reported as means ± standard deviations. A one-way analysis of variance (ANOVA) was performed with a Tukey's *post hoc* test to assess statistical significance with $n = 5$ cords. Statistical significance was set at $p < 0.05$.

Results and Discussion

As hypothesized, hUCMSCs treated with RI displayed significantly increased survival rates and transfection efficiencies after nucleofection than hUCMSCs that were not treated with RI. Gene delivery is a powerful tool for reprogramming hUCMSCs as demonstrated by Baksh et al. (2007) and Devarajan et al. (2013). Until now, nonviral delivery methods have suffered from poor transfection efficiency with high cell viability or high transfection efficiency with poor cell viability. RhoA GTP signaling pathways are critical for inducing several apoptotic mechanisms in response to unfavorable environmental changes (Ichikawa et al., 2013; Ohgushi et al., 2010). Inhibiting ROCK can reduce apoptosis associated with detachment and freezing protocols (Harb et al., 2008; Ichikawa et al., 2012; Koyanagi et al., 2008; Kurosawa, 2012; Olson, 2008). One of the key disadvantages

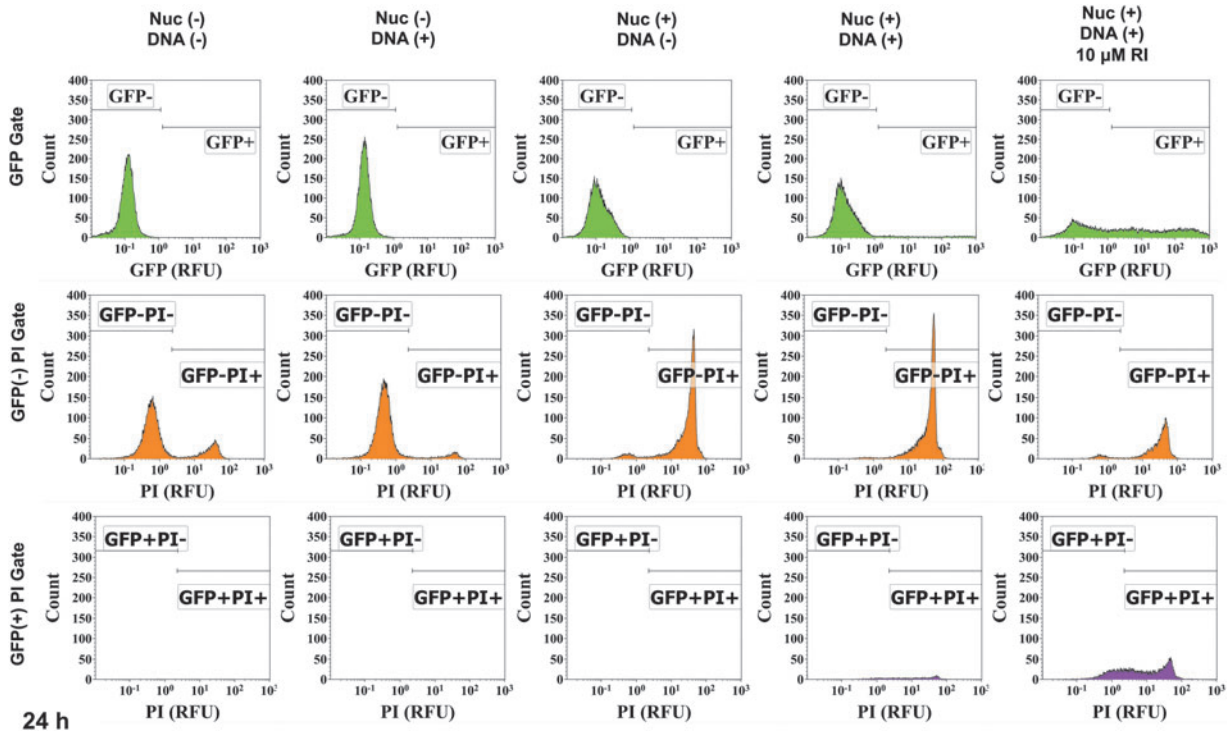

FIG. 1. Flow cytometry gating parameters used to quantify cell numbers. The set of histograms displayed are an arbitrary selection of a single replicate for each treatment from one umbilical cord out of five tested. Nuc (+/−) designates whether cells were Nucleofected™ or not. DNA (+/−) designates whether cells received 5 μg of pmaxGFP or not. RFU, relative fluorescence units; RI, ROCK Inhibitor. Color images available online at www.liebertpub.com/cell

Table 1. Gating Statistics

Treatment	Replicate	Cell number from gate	GFP (+)		GFP (−)	
			Live	Dead	Live	Dead
Nuc (−)	A	18,811	0.0%	0.0%	91.2%	8.8%
DNA (−)	B	19,297	0.0%	0.0%	97.0%	3.0%
	C	19,571	0.0%	0.0%	96.9%	3.1%
	Mean	19,226 ± 385	0.0%	0.0%	95.0 ± 3.3%	5.0 ± 3.3%
Nuc (−)	A	18,805	0.0%	0.0%	11.9%	88.1%
DNA (+)	B	18,933	0.0%	0.0%	12.1%	97.9%
	C	18,989	0.0%	0.0%	10.1%	89.9%
	Mean	18,909 ± 94	0.0%	0.0%	11.4 ± 1.1%	92.0 ± 5.2%
Nuc (+)	A	19,753	0.0%	0.0%	93.3%	6.7%
DNA (−)	B	19,756	0.0%	0.0%	96.9%	3.2%
	C	19,738	0.0%	0.0%	97.0%	3.0%
	Mean	19,749 ± 10	0.0%	0.0%	95.7 ± 2.1%	4.3 ± 2.1%
Nuc (+)	A	19,323	0.2%	5.0%	1.9%	92.9%
DNA (+)	B	19,178	1.4%	4.7%	1.4%	92.6%
	C	19,161	1.2%	3.8%	1.4%	93.6%
	Mean	19,221 ± 89	0.93 ± 0.64%	4.5 ± 0.62%	1.6 ± 0.32%	93.0 ± 0.53%
Nuc (+)	A	19,033	16.5%	36.3%	3.8%	43.4%
DNA (+)	B	19,298	25.8%	29.8%	7.9%	36.5%
10 μM RI	C	18,876	8.2%	29.6%	2.6%	59.6%
	Mean	19,069 ± 213	16.8 ± 8.8%	31.9 ± 3.8%	4.8 ± 2.8%	46 ± 12%

RI, Rock Inhibitor.

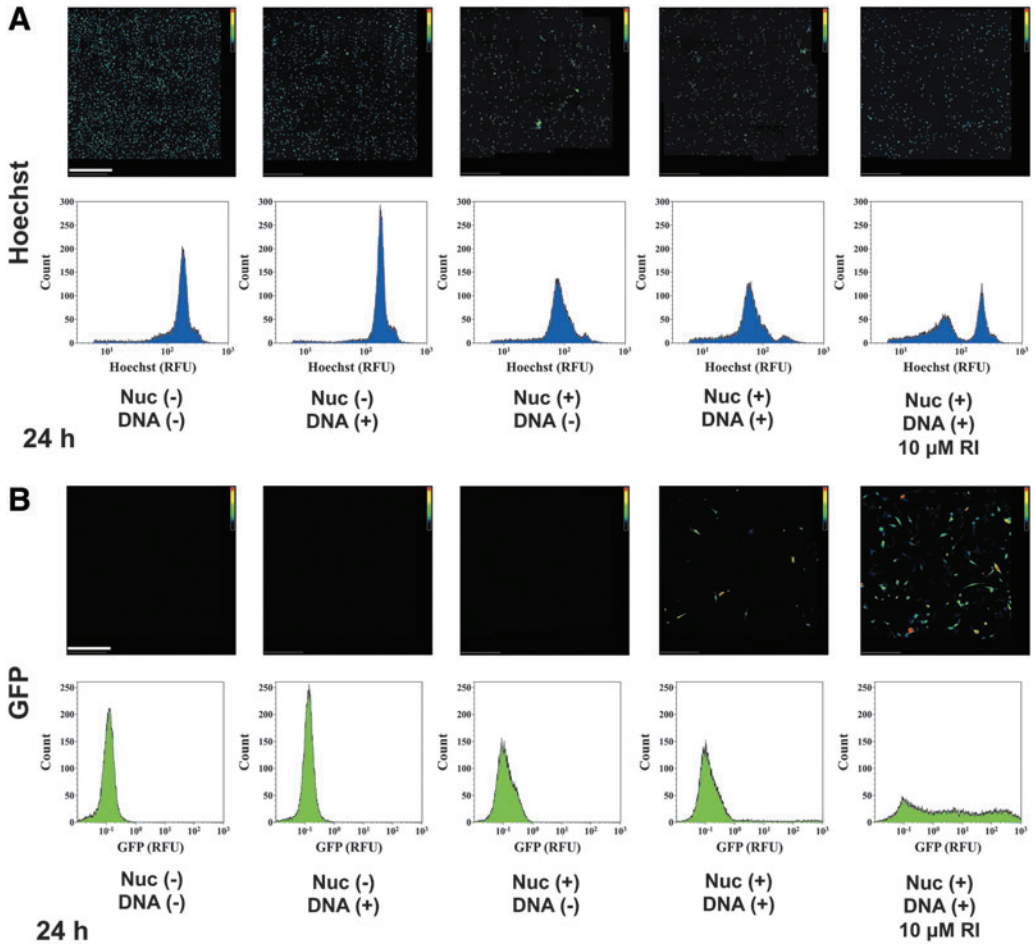

FIG. 2. (**A**) Intensity maps of cell density with corresponding flow cytometry histograms of Hoechst signal distribution 24 h after transfection. (**B**) Intensity maps of GFP expression with corresponding flow cytometry histograms of GFP expression 24 h after transfection. The set of images and corresponding histograms are an arbitrary selection from one cord out of five tested. Nuc (+/−) designates whether cells were Nucleofected™ or not. DNA (+/−) designates whether cells received 5 μg of pmaxGFP or not. Scale bar, 500 μm. RFU, relative fluorescence units; GFP, green fluorescent protein; RI, ROCK Inhibitor. Color images available online at www.liebertpub.com/cell

of using nonviral physical delivery methods such as electroporation is the need to dissociate cells from adherent surfaces. However, by using Y-27632-RI to mitigate some of the apoptotic mechanisms induced by cell detachment and electric shock, it might be possible to rescue positively transfected cells from cell death, which was the primary goal of this study.

Flow cytometry analysis revealed that the cell populations were mostly nonhematopoietic because the hUCMSCs were 98.1 ± 0.04% negative for CD34 expression and 90.4 ± 1.1% negative for CD45 expression. The expression of CD90, a key mesenchymal stem cell marker, was detected in 98.5 ± 0.54% of cells. The expression of remaining key mesenchymal stem cell markers, CD73 (12.0 ± 7.8%), CD105 (10.2 ± 0.15%), and STRO-1 (3.4 ± 0.33%), were low and relatively variable, suggesting subpopulations may exist within each cell population that displayed surface epitopes consistent with mesenchymal stem cell markers, as reviewed by (Wang et al., 2009; Wang et al., 2011).

As was seen in the microscopy images at 24 h (Fig. 2A) and 48 h (Fig. 3A) after transfection, hUCMSCs that were not subjected to nucleofection displayed high cell densities compared to hUCMSCs that were subject to nucleofection. However, hUCMSCs that were treated with 10 μM of Y-27632-RI before and after transfection displayed a greater cell density than hUCMSCs that were subject to nucleofection and not treated with Y-27632-RI, as shown in microscopy images and corroborated by flow cytometry data.

There was a clear increase in both cell viability and transfection efficiency between the experimental group of hUCMSCs that was nucleofected and treated with Y-27632-RI and the group of hUCMSCs that was nucleofected and not treated with Y-27632-RI at both 24 h and 48 h after transfection (Fig. 4). Cell viability was 3.3 times greater in hUCMSCs treated with Y-27632-RI than hUCMSCs that were not treated with Y-27632-RI 24 h after transfection ($p < 0.05$), whereas cell viability was 3.2 times greater in hUCMSCs treated with Y-27632-RI than hUCMSCs not treated with Y-27632-RI 48 h after transfection ($p < 0.01$). Transfection efficiency was 4.6 times greater in hUCMSCs treated with Y-27632-RI than hUCMSCs not treated with Y-27632-RI 24 h after transfection ($p < 0.01$). At 48 h after transfection, transfection efficiency was 4.8 times greater in hUCMSCs treated with Y-27632-RI than hUCMSCs not treated with Y-27632-RI ($p < 0.05$).

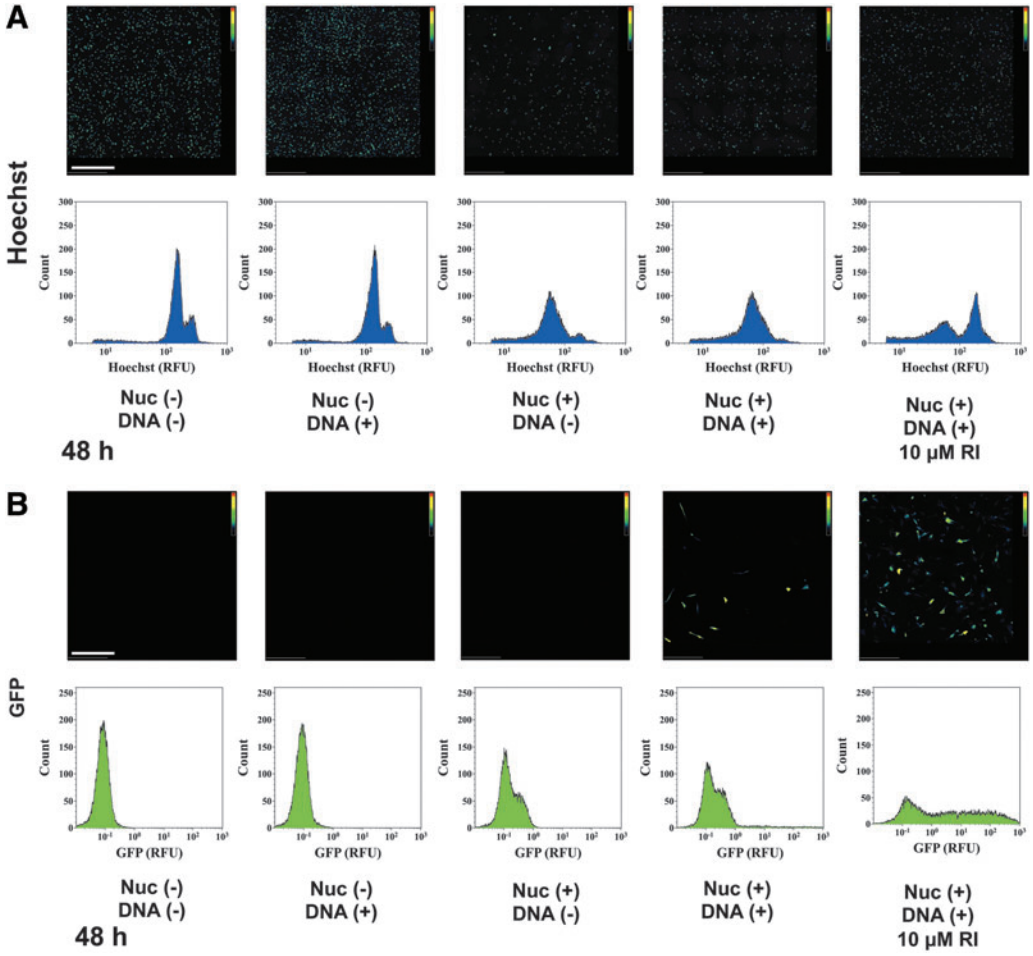

FIG. 3. (**A**) Intensity maps of cell density with corresponding flow cytometry histograms of Hoechst signal distribution 48 h after transfection. (**B**) Intensity maps of GFP expression with corresponding flow cytometry histograms of GFP expression 48 h after transfection. The set of images and corresponding histograms are an arbitrary selection from one cord out of five tested. Nuc (+/−) designates whether cells were Nucleofected™ or not. DNA (+/−) designates whether cells received 5 μg of pmaxGFP or not. Scale bar, 500 μm. RFU, relative fluorescence units; GFP, green fluorescent protein; RI, ROCK Inhibitor. Color images available online at www.liebertpub.com/cell

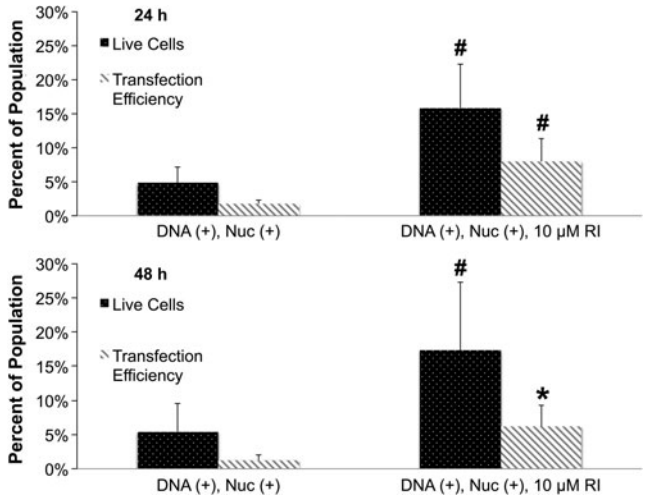

FIG. 4. Live/dead and transfection efficiency collected via flow cytometry 24 h and 48 h after transfection. Groups that did not express GFP were not plotted in the bar chart. (*) Statistically significant difference ($p < 0.05$) from hUCMSCs that underwent Nucleofection™ without RI supplement; (#) statistically significant difference ($p < 0.01$) from hUCMSCs that underwent Nucleofection™ without RI supplement. The results are representative of cells collected from five different umbilical cords ($n = 5$) and are reported as statistical means. All experiments were repeated three times. Error bars represent standard deviations. Nuc (+/−) designates whether cells were Nucleofected™ or not. DNA (+/−) designates whether cells received 5 μg of pmaxGFP or not. RI, ROCK Inhibitor.

The difference in GFP intensity may have been a result of an increased number of live cells present and able to readhere to a surface when treated with Y-27632-RI as opposed to hUCMSCs that were not treated with Y-27632-RI. The flow cytometry histograms were consistent with microscopy images in showing that a greater number of hUCMSCs treated with Y-27632-RI survived and expressed GFP at varying intensities at both 24 h (Fig. 2B) and 48 h (Fig. 3B) after transfection than hUCMSCs that were not treated with Y-27632-RI. Furthermore, the data from the histograms suggested that there might be a relationship between GFP expression and cell density. Further formal studies are needed to verify if an actual relationship exists.

hUCMSCs treated with Y-27632-RI at both 24 h and 48 h post-transfection displayed an increase in cell viability and a far more substantial increase in transfection efficiency compared to hUCMSCs that were not treated with Y-27632-RI. Thus, future studies are needed to explore whether a synergistic phenomenon is occurring in which Y-27632-RI is not only rescuing dying cells, but also improving cell health to facilitate expression of GFP in cells that may not have been previously able to express GFP. Further long-term studies are needed to determine whether Y-27632-RI can prolong and sustain gene expression in hUCMSCs. Additionally, follow-up studies are needed to determine whether Y-27632-RI can negatively affect multipotency character and downstream differentiation of hUCMSCs for tissue engineering applications (Watanabe et al., 2007; Pakzad et al., 2010).

For the first time, it was demonstrated that Y-27632-RI enhanced survival and gene expression in mesenchymal stromal cells for an electroporative gene delivery strategy. Transfection efficiency significantly increased four-fold and cell viability increased three-fold in hUCMSC populations that were treated with 10 μM of Y-27632-RI before and after transfection compared to hUCMSC populations not treated with Y-27632-RI. Although this study focused on hUCMSCs and provides an example for evaluating the effect of Y-27632-RI, other cell types undergoing electroporation may benefit from Y-27632-RI treatment, although dosing levels, application of treatment, and timing of treatment should be tailored for each cell type and application. The use of Y-27632-RI provides an opportunity to benefit strategies that combine both stem cell therapy and gene therapy for regenerative medicine applications.

Acknowledgments

We would like to acknowledge the efforts of the nursing staffs at the University of Kansas Hospital (Kansas City, KS), Lawrence Memorial Hospital (Lawrence, KS), and Stormont-Vail (Topeka, KS) for assisting us in obtaining human umbilical cords. Furthermore, we would like to acknowledge the efforts of Peggy Keefe and Austin Smith for their assistance on this project. This project was funded by the National Institutes of Health (NIH) and the state of Kansas.

Author Disclosure Statement

The authors declare that there are no conflicts of interest.

References

Andre, F.M., and Mir, L.M. (2010). Nucleic acids electrotransfer in vivo: Mechanisms and practical aspects. Curr Gene Ther 10, 267–280.

Bailey, M., Wang, L., Bode, C., Mitchell, K., and Detamore, M. (2007a). A comparison of human umbilical cord matrix stem cells and temporomandibular joint condylar chondrocytes for tissue engineering temporomandibular joint condylar cartilage. Tiss. Eng. 13, 2003–2010.

Baksh, D., Yao, R., and Tuan, R.S. (2007). Comparison of proliferative and multilineage differentiation potential of human mesenchymal stem cells derived from umbilical cord and bone marrow. Stem Cells 25, 1384–1392.

Chatterjee, P., Cheung, Y., and Liew, C. (2011). Transfecting and nucleofecting human induced pluripotent stem cells. J. Vis. Exp. Oct 5;(56). pii: 3110. doi: 10.3791/3110.

Check, E. (2005). Gene therapy put on hold as third child develops cancer. Nature 433, 561.

Claassen, D.A., Desler, M.M., and Rizzino, A. (2009). ROCK inhibition enhances the recovery and growth of cryopreserved human embryonic stem cells and human induced pluripotent stem cells. Mol. Reprod. Dev. 76, 722–732.

Devarajan, K., Forrest, M.L., Detamore, M.S., and Staecker, H. (2013). Adenovector-mediated gene delivery to human umbilical cord mesenchymal stromal cells induces inner ear cell phenotype. Cell. Reprogram. 15, 43–54.

Ear, T., Giguere, P., Fleury, A., Stankova, J., Payet, M.D., and Dupuis, G. (2001). High efficiency transient transfection of genes in human umbilical vein endothelial cells by electroporation. J. Immunol. Methods 257, 41–49.

Emre, N., Vidal, J.G., Elia, J., O'Connor, E.D., Paramban, R.I., Hefferan, M.P., Navarro, R., Goldberg, D.S., Varki, N.M., Marsala, M., and Carson, C.T. (2010). The ROCK inhibitor

Y-27632 improves recovery of human embryonic stem cells after fluorescence-activated cell sorting with multiple cell surface markers. PloS One 5, e12148.

Gauthaman, K., Fong, C.Y., and Bongso, A. (2010a). Effect of ROCK inhibitor Y-27632 on normal and variant human embryonic stem cells (hESCs) in vitro: Its benefits in hESC expansion. Stem Cell Rev. 6, 86–95.

Gauthaman, K., Fong, C.Y., Subramanian, A., Biswas, A., and Bongso, A. (2010b). ROCK inhibitor Y-27632 increases thaw-survival rates and preserves stemness and differentiation potential of human Wharton's jelly stem cells after cryopreservation. Stem Cell Rev. 6, 665–676.

Golzio, M., Escoffre, J.M., Portet, T., Mauroy, C., Teissie, J., Dean, D.S., and Rols, M.P. (2010). Observations of the mechanisms of electromediated DNA uptake—from vesicles to tissues. Curr. Gene Ther. 10, 256–266.

Harb, N., Archer, T., and Sato, N. (2008). The Rho-Rock-Myosin signaling axis determines cell-cell integrity of self-renewing pluripotent stem cells. PloS One 3, e3001.

Ichikawa, H., Nakata, N., Abo, Y., Shirasawa, S., Yokoyama, T., Yoshie, S., Yue, F., Tomotsune, D., and Sasaki, K. (2012). Gene pathway analysis of the mechanism by which the Rho-associated kinase inhibitor Y-27632 inhibits apoptosis in isolated thawed human embryonic stem cells. Cryobiology 64, 12–22.

Ichikawa, H., Kanoh, Y., Shirasawa, S., Yokoyama, T., Yue, F., Tomotsune, D., and Sasaki, K. (2013). Unique kinetics of Oct3/4 microlocalization following dissociation of human embryonic stem cell colonies. Ann. Anat. 195, 50–56.

Jang, J.H., Houchin, T.L., and Shea, L.D. (2004). Gene delivery from polymer scaffolds for tissue engineering. Expert Rev. Med. Devices 1, 127–138.

Joo, H., Choi, D.-K., Lim, J., Park, J.-S., Lee, S.-H., Song, S., Shin, J., Lim, D.-S., Kim, I., Hwang, K.-C., and Koh, G.Y. (2012). ROCK suppression promotes differentiation and expansion of endothelial cells from embryonic stem cell-derived Flk1(+) mesodermal precursor cells. Blood 120, 2733–2744.

Kofron, M.D., and Laurencin, C.T. (2006). Bone tissue engineering by gene delivery. Adv. Drug Deliv. Rev. 58, 555–576.

Koyanagi, M., Takahashi, J., Arakawa, Y., Doi, D., Fukuda, H., Hayashi, H., Narumiya, S., and Hashimoto, N. (2008). Inhibition of the Rho/ROCK pathway reduces apoptosis during transplantation of embryonic stem cell-derived neural precursors. J. Neurosci. Res. 86, 270–280.

Kurosawa, H. (2012). Application of Rho-associated protein kinase (ROCK) inhibitor to human pluripotent stem cells. J. Biosci. Bioeng. 114, 577–581.

Mellott, A.J., Forrest, M.L., and Detamore, M.S. (2013). Physical non-viral gene delivery methods for tissue engineering. Ann. Biomed. Eng. 41, 446–468.

Narumiya, S., Ishizaki, T., and Uehata, M. (2000). Use and properties of ROCK-specific inhibitor Y-27632. Methods Enzymol. 325, 273–284.

Ohgushi, M., and Sasai, Y. (2011). Lonely death dance of human pluripotent stem cells: ROCKing between metastable cell states. Trends Cell Biol. 21, 274–282.

Ohgushi, M., Matsumura, M., Eiraku, M., Murakami, K., Aramaki, T., Nishiyama, A., Muguruma, K., Nakano, T., Suga, H., Ueno, M., Ishizaki, T., Suemori, H., Narumiya, S., Niwa, H., and Sasai, Y. (2010). Molecular pathway and cell state responsible for dissociation-induced apoptosis in human pluripotent stem cells. Cell Stem Cell 7, 225–239.

Olson, M.F. (2008). Applications for ROCK kinase inhibition. Curr. Opin. Cell Biol. 20, 242–248.

Pakzad, M., Totonchi, M., Taei, A., Seifinejad, A., Hassani, S.N., and Baharvand, H. (2010). Presence of a ROCK inhibitor in extracellular matrix supports more undifferentiated growth of feeder-free human embryonic and induced pluripotent stem cells upon passaging. Stem Cell Rev. 6, 96–107.

Shi, J., Wu, X., Surma, M., Vemula, S., Zhang, L., Yang, Y., Kapur, R., and Wei, L. (2013). Distinct roles for ROCK1 and ROCK2 in the regulation of cell detachment. Cell Death Dis. 4, e483.

Shin, S., Salvay, D.M., and Shea, L.D. (2010). Lentivirus delivery by adsorption to tissue engineering scaffolds. J. Biomed. Mater. Res. A 93:1252–1259.

Thomas, C.E., Ehrhardt, A., and Kay, M.A. (2003). Progress and problems with the use of viral vectors for gene therapy. Nat. Rev. Genet. 4, 346–358.

Wang, L., Tran, I., Seshareddy, K., Weiss, M.L., and Detamore, M.S. (2009). A comparison of human bone marrow-derived mesenchymal stem cells and human umbilical cord-derived mesenchymal stromal cells for cartilage tissue engineering. Tiss. Eng. Part A 15, 2259–2266.

Wang, L., Ott, L., Seshareddy, K., Weiss, M.L., and Detamore, M.S. (2011). Musculoskeletal tissue engineering with human umbilical cord mesenchymal stromal cells. Regen. Med. 6, 95–109.

Watanabe, K., Ueno, M., Kamiya, D., Nishiyama, A., Matsumura, M., Wataya, T., Takahashi, J.B., Nishikawa, S., Nishikawa, S., Muguruma, K., and Sasai, Y. (2007). A ROCK inhibitor permits survival of dissociated human embryonic stem cells. Nat. Biotechnol. 25, 681–686.

Weiss, M.L., and Troyer, D. (2008). Stem cells in the umbilical cord. Stem Cell Reviews 6, 155–162.

Xu, B., Song, G., Ju, Y., Li, X., Song, Y., and Watanabe, S. (2012). RhoA/ROCK, cytoskeletal dynamics, and focal adhesion kinase are required for mechanical stretch-induced tenogenic differentiation of human mesenchymal stem cells. J. Cell. Physiol. 227, 2722–2729.

Zhang, K., Zhang, H., Xiang, H., Liu, J., Liu, Y., Zhang, X., Wang, J., and Tang, Y. (2013). TGF-β1 induces the dissolution of tight junctions in human renal proximal tubular cells: Role of the RhoA/ROCK signaling pathway. Int. J. Mol. Med. 32, 464–468.

Zhang, L., Valdez, J.M., Zhang, B., Wei, L., Chang, J., and Xin, L. (2011). ROCK inhibitor Y-27632 suppresses dissociation-induced apoptosis of murine prostate stem/progenitor cells and increases their cloning efficiency. PloS One 6, e18271.

Zhang, X., and Godbey, W.T. (2006). Viral vectors for gene delivery in tissue engineering. Adv. Drug Deliv. Rev. 58, 515–534.

Zimmermann, U. (1982). Electric field-mediated fusion and related electrical phenomena. Biochim. Biophys. Acta 694, 227–277.

Address correspondence to:
Michael S. Detamore
University of Kansas
Department of Chemical and Petroleum Engineering
4163 Learned Hall, 1530 W 15th St
Lawrence, KS 66045

E-mail: detamore@ku.edu